Proc. Natl. Acad. Sci. USA
Vol. 96, pp. 3059–3064, March 1999
Medical Sciences

Poly(ADP-ribose) polymerase-deficient mice are protected from streptozotocin-induced diabetes

ANDREW A. PIEPER*, DANIEL J. BRAT†, DAVID K. KRUG*, CRYSTAL C. WATKINS*, ALOK GUPTA*, SETH BLACKSHAW*, AJAY VERMA‡, ZHAO-QI WANG§, AND SOLOMON H. SNYDER*¶

*Departments of Neuroscience, Pharmacology and Molecular Sciences, and Psychiatry, and †Department of Pathology, The Johns Hopkins University School of Medicine, 725 North Wolfe Street, Baltimore, MD 21205; ‡Uniformed Services University of the Health Sciences, 4301 Jones Bridge Road, Bethesda, MD 20814; and §International Agency for Research on Cancer, 150, cours Albert Thomas, F-69008 Lyon, France

Contributed by Solomon H. Snyder, December 31, 1998

ABSTRACT **Streptozotocin (STZ) selectively destroys insulin-producing beta islet cells of the pancreas providing a model of type I diabetes. Poly(ADP-ribose) polymerase (PARP) is a nuclear enzyme whose overactivation by DNA strand breaks depletes its substrate NAD^+ and then ATP, leading to cellular death from energy depletion. We demonstrate DNA damage and a major activation of PARP in pancreatic islets of STZ-treated mice. These mice display a 500% increase in blood glucose and major pancreatic islet damage. In mice with homozygous targeted deletion of PARP (PARP −/−), blood glucose and pancreatic islet structure are normal, indicating virtually total protection from STZ diabetes. Partial protection occurs in PARP +/− animals. Thus, PARP activation may participate in the pathophysiology of type I diabetes, for which PARP inhibitors might afford therapeutic benefit.**

Type I diabetes (insulin-dependent diabetes mellitus) is a chronic metabolic disorder characterized by a loss of pancreatic islet B cell mass, decreased serum insulin, and hyperglycemia. Although the pathogenic mechanisms of this disease have not been fully characterized, genetic, environmental, and autoimmune factors have been postulated. In particular, development of this disorder is postulated to proceed through generation of oxygen radicals during prediabetic pancreatic islet inflammation (1, 2). One possible mechanism is that autoimmune activation of macrophages damages B cells through release of massive amounts of NO after inducible NO synthase activation, as damage elicited when islets are cocultured with macrophages is prevented by inhibition of NO synthase (3).

Focal cerebral ischemic damage is also associated with NO release leading to DNA damage elicited by reactive oxygen species, including peroxynitrite formed from NO. Downstream of this DNA damage, the enzyme poly(ADP-ribose) polymerase (PARP, EC 2.4.2.30) is stimulated. Nuclear PARP is activated by DNA fragments to transfer branched chains of up to 200 ADP ribose groups from NAD^+ to acceptor proteins in the nucleus, including histones and PARP itself. PARP activation plays a role in DNA repair, particularly the base excision repair process (4–8), in response to moderate amounts of DNA damage. With excessive DNA damage, however, PARP is so highly activated that its substrate NAD^+ is critically depleted (9). NAD^+ is an important enzyme in energy metabolism, and its depletion results in lower ATP production. As ATP is also consumed in efforts to resynthesize NAD^+, cells can die from energy loss. Cerebral ischemic damage is greatly diminished in mice with targeted deletion of PARP (PARP −/−) (10, 11) and in animals treated with PARP inhibitors (12, 13). A role of PARP activation in pancreatic damage is also suggested by protection through PARP inhibition of pancreatic islet cells from NO-mediated killing (14, 15). Furthermore, *in vitro* pancreatic islet cells from PARP −/− mice are resistant to NAD^+ depletion after exposure to either NO or other reactive oxygen intermediates generated through the oxidation of hypoxanthine by xanthine oxidase (16).

Streptozotocin (STZ)-induced diabetes in mice and rats has been used widely as an animal model to study type I diabetes (17, 18). A single large dose of STZ is sufficient to induce hyperglycemia resulting from loss of pancreatic B cells. This alkylating agent induces high levels of DNA strand breaks in B cells, causing activation of PARP, resultant reduction of cellular NAD^+, and cell death (19–21). Cotreatment of mice with nicotinamide, a PARP inhibitor and precursor of NAD^+, attenuates STZ-induced diabetes (22). To further elucidate the role of PARP activation in STZ-induced diabetes, we have used heterozygous and homozygous PARP knockout mice. In this aim we have developed two new techniques for studying DNA damage. Enhanced DNA *p*olymerase I-mediated digoxygenin-d*U*TP *n*ick-*t*ranslation (PUNT+) is a highly sensitive technique for detecting single-stranded DNA breaks *in situ*. This technique is sufficiently sensitive to detect damage not only in the context of cell death but in the context of basal DNA damage as well. Basal damage may involve mitochondrial and/or nuclear DNA. These forms of DNA damage can be distinguished by their relative intensity. The technique of *p*oly(*A*DP-*r*ibose) *in situ* (PARIS) detection allows rapid and specific visual localization of PARP activation in fresh-frozen tissue through autoradiographic monitoring of the conversion of $[^{33}P]NAD^+$ to poly(ADP-ribose) polymer.

MATERIALS AND METHODS

STZ Administration. Male PARP −/−, PARP +/−, and wild-type 129/SV mice (Taconic Farms) were injected at age 10 weeks. STZ (Sigma) was dissolved at 10 mg/ml in 0.1 M sodium citrate buffer (pH 5.5) and injected i.p. into mice at a dose of 200 mg/kg. Control mice were injected with vehicle only. Mice were allowed free access to food and water. Mice were killed by cervical dislocation.

Blood Glucose Measurement. Mouse tail vein blood glucose levels were monitored weekly after 12–18 h of fasting by analysis with the Boehringer Mannheim Accu-Chek Easy blood glucose monitor model no. 788.

Immunohistochemistry. Six weeks after STZ injection, mouse pancreata from each treatment group were dissected

The publication costs of this article were defrayed in part by page charge payment. This article must therefore be hereby marked "*advertisement*" in accordance with 18 U.S.C. §1734 solely to indicate this fact.

PNAS is available online at www.pnas.org.

Abbreviations: PARP, poly(ADP ribose) polymerase; STZ, streptozotocin; PUNT+, enhanced DNA polymerase I-mediated digoxygenin-dUTP nick translation; PARIS, poly(ADP ribose) *in situ*; TBS, Tris-buffered saline; HRP, horseradish peroxidase; RT, room temperature; SSPE, standard saline phosphate/EDTA.

¶To whom reprint requests should be addressed. e-mail: ssnyder@jhmi.edu.

and immediately fixed in 4% buffered formalin. Tissue was paraffin-embedded and routinely sectioned (10 μm) for staining with hematoxylin/eosin and by immunohistochemistry. For immunostaining, slides were incubated overnight at room temperature (RT) with primary antibodies against human insulin (monoclonal, 1:1,000; Dako) or glucagon (monoclonal, 1:1,500 Dako). Biotinylated goat anti-rabbit (Vector Laboratories) antibody was used as the secondary antibody, and signal was amplified with an ABC kit (Vector Laboratories) using diaminobenzidine as a chromogen.

Western Blot for PARP. Freshly dissected mouse pancreas was homogenized in Nonidet P-40 lysis buffer, sonicated for 15 sec, and normalized for protein content with the bicinchoninic acid protein assay (Pierce). Pancreatic protein (20 μg) was resolved by SDS/PAGE in each lane of a 4–12% gradient gel and then transferred to nitrocellulose membrane. To detect PARP protein, the nitrocellulose membrane was probed with rabbit anti-PARP antibody [BioMol, Plymouth Meeting, PA; 1:3500 dilution in 3% BSA/Tris-buffered saline (TBS)] for 2 h at RT with gentle agitation, followed by three 5-min washes with 0.5% BSA/TBS and subsequent incubation with goat anti-rabbit horseradish peroxidase-conjugated secondary antibody (Amersham Life Science, 1:15,000 dilution in 3% BSA/TBS) for 45 min at RT. Labeled protein was visualized through enhanced chemiluminescence with Renaissance Western Blot Chemiluminescence Reagent Plus (NEN Life Science Products).

Enhanced DNA PUNT+. This protocol was derived from refs. 23 and 24, with modifications by S.B. Cryostat sections (20 μm) of fresh frozen pancreata were cut onto Superfrost Plus slides. Sections were fixed in 4% paraformaldehyde in PBS for 20 min, washed three times for 3 min in 2× standard saline phosphate/EDTA (SSPE; 1× SSPE = 0.13 NaCl/10 mM phosphate, pH 7.4/1 mM EDTA), and then permeabilized for 20 min in 2× SSPE, 0.5% Triton X-100. Slides were washed two times for 3 min in 2× SSPE, acetylated 10 min in 0.1 M triethanolamine (pH 8.0), and then washed three times for 3 min in 2× SSPE. Sections were dehydrated through an ethanol series and allowed to dry at RT. Each section was covered with 500 μl of reaction mix [0.5 mM dATP, dCTP, dGTP, and digoxygenin-11-dUTP (Boehringer Mannheim)/7.5 units/ml DNA polymerase I (Sigma)] in PBS buffer containing 5 mm $MgCl_2$, 10 mM 2-mercaptoethanol, and 20 mg/ml BSA. Negative controls that omitted either DNA polymerase I or the digoxygenin-labeled nucleotide failed to show any signal. Slides were incubated at 37°C for 1 h in a humidified chamber. The reaction was stopped by incubating slides at 65°C in 2× SSPE for 2 h. Slides were then washed three times for 5 min in TBS. Nonspecific immunoreactivity was blocked by incubating slides with 5% normal goat serum in TBS for 1 h at RT. Slides were incubated overnight at RT in the same blocking buffer containing anti-digoxygenin Fab fragment-AP (Boehringer Mannheim) at 1:5000 dilution. Slides were then washed three times for 5 min in TBS and incubated for 5 min in alkaline phosphatase buffer (0.1 M Tris·HCl, pH 9.5/0.1 M NaCl/50 mM $MgCl_2$). The color reaction was conducted by incubating slides in alkaline phosphatase reaction solution [alkaline phosphatase buffer with 3.375 μl/ml nitroblue tetrazolium (Boehringer Mannheim)/3.5 μl/ml 5-bromo-4-chloro-3′-indolylphosphate P-toluidine salt (Boehringer Mannheim)/0.24 mg/ml levamisole (Sigma)]. The color reaction was allowed to proceed for 1 h. The reaction was stopped by incubating slides in buffer. Slides were coverslipped with Aquapolymount (Polysciences).

PARIS Detection. Fresh-frozen cryostat sections from mouse pancreas (10 μm) were allowed to warm to RT and then preincubated at RT in PARIS buffer (56 mM Hepes/28 mM KCl/28 mM NaCl/5 mM $MgCl_2$/0.01% digitonin/2 mM DTT/1 mM novobiocin, pH 7.5) for 15 min. In control sections, 1 mM benzamide was added to inhibit PARP activity. Liquid was then carefully aspirated by using a gentle vacuum so as not to disturb the tissue. Sections were then covered with 200 μl of PARIS buffer containing 30 nM [^{33}P]NAD$^+$ (NEN Life Science Products) and incubated at 4°C for 15 min. After incubation, the slides were transferred into staining jars containing 10% trichloroacetic acid at 4°C for 10 min and then dried under a cool stream of air. For autoradiography, sections were dipped into a 50% solution of Kodak NBT2 emulsion in a darkroom, allowed to dry, and exposed for 3–5 days. Sections were developed for 5 min by using Kodak D19 developer and then fixed for 5 min in Kodak rapid fixer.

Quantification of PARIS Signal. Sections adjacent to those used for PARIS and PUNT+ visualization were subjected to PARIS and then scraped into solubilization buffer (2% SDS/0.1 M NaOH), normalized for protein content with the bicinchoninic acid protein assay (Pierce), and subjected to scintillation counting of radioactively labeled poly(ADP-ribose). Protein content and scintillation quantification were obtained in triplicate and averaged for each sample.

RESULTS

Within 1 week after STZ treatment, blood glucose levels in wild-type animals increase ≈5-fold and later peak at levels about eight times the control values (Fig. 1). PARP −/− mice display no hyperglycemia with glucose levels essentially the same as those of wild-type animals. Partial protection occurs in heterozygotes whose blood glucose levels at 1 week are the same as those of PARP −/− animals, although at 2 weeks they have increased to the value of wild-type mice injected with STZ. Thus the onset of diabetes in heterozygotes appears to be delayed but not prevented. Both PARP +/− and wild-type mice treated with STZ show transiently decreased hyperglycemia at weeks 3 and 4, with the establishment of stable and

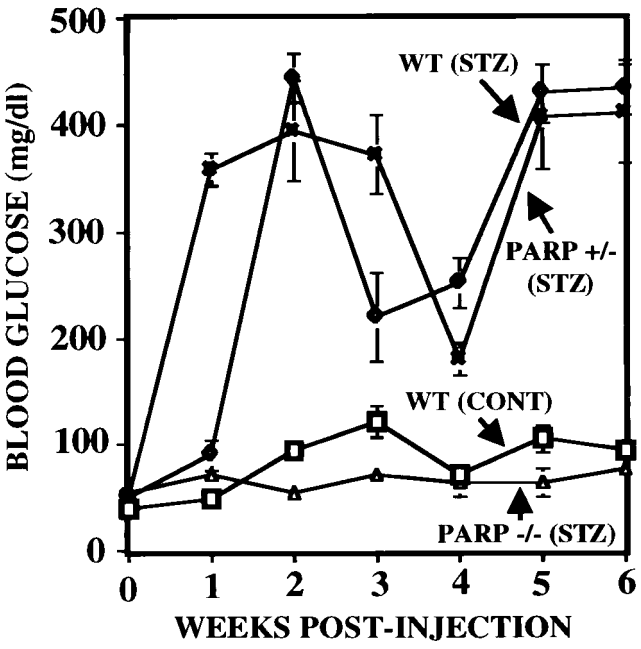

FIG. 1. PARP −/− mice are protected from STZ-induced hyperglycemia. Within 1 week of i.p. injection of 200 mg/kg STZ, wild-type mice show markedly elevated blood glucose that peaks at 2 weeks and remains elevated at 6 weeks. PARP −/− mice do not become hyperglycemic after injection but rather show a blood glucose profile that parallels that of control wild-type mice injected with vehicle only. PARP +/− mice show no increase in blood glucose at 1 week, but at 2 weeks they become as hyperglycemic as treated wild-type mice and remain hyperglycemic 6 weeks after injection. Values are means ± SEM for three trials with at least 5 mice per group.

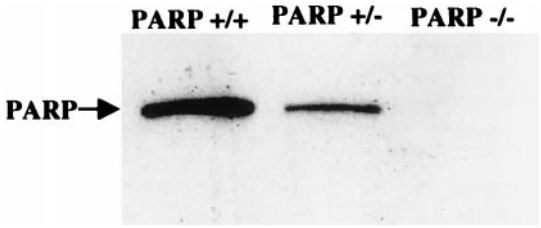

FIG. 2. Western blot analysis of pancreatic proteins with anti-PARP antibody shows that PARP protein is absent from pancreas of PARP −/− mice and abundant in PARP +/+ pancreas. PARP +/− pancreas shows approximately half of the PARP +/+ level of PARP protein. The blot shown is typical of four independent replications.

dramatic hyperglycemia after week 5. Delayed onset of hyperglycemia in heterozygotes may reflect the diminished PARP protein levels observed by Western blot analysis in heterozygotes. Although no PARP protein is detectable in PARP −/− pancreas, PARP levels are reduced ≈50% in PARP +/− animals (Fig. 2).

Microscopic examination of the pancreas explains the PARP −/− resistance to STZ-induced hyperglycemia (Fig. 3). In wild-type mice treated with STZ, the number of islet cells is greatly reduced, whereas remaining islets are smaller and distorted in appearance with many fewer cells staining for insulin. Glucagon-staining α cells account for a major proportion of residual islet cell mass, consistent with selectivity of STZ for B cells. In striking contrast, PARP −/− islets are completely protected from this damage with overall morphology and staining for insulin and glucagon being indistinguishable from wild-type controls. Heterozygotes display islet damage and diminished insulin staining comparable with wild-type mice treated with STZ.

The remarkable protection of PARP −/− mice from STZ-diabetes implies that STZ elicits DNA damage that overactivates PARP. The DNA damage may be elicited by a number of mechanisms, including direct alkylation of DNA as well as generation of an immune response against pancreatic islet B cells (25). PUNT+ staining reveals that STZ markedly augments DNA damage with similar augmentation in wild-type, PARP +/−, and PARP −/− pancreas (Fig. 4). Furthermore, untreated PARP +/− and PARP −/− mice exhibit markedly elevated levels of accumulated DNA strand breaks in pancreatic islet cells (Fig. 4). This increased accumulation of DNA breaks in PARP +/− and PARP −/− pancreas corresponds with recent studies suggesting a critical role for PARP in normal base excision repair (4–8).

PARP activation elicited in wild-type animals by STZ treatment is abolished in PARP −/− mice (Fig. 5). STZ augments whole-pancreatic PARP activity in wild-type animals by ≈60%. PARP activity in PARP +/− pancreas is ≈40% levels of wild-type animals and increases ≈50% after treatment with STZ. Only negligible PARP activity is detected in PARP −/− pancreas with or without STZ treatment.

Islet cells constitute only a small percentage of pancreatic tissue so that augmentation of PARP activity in the whole pancreas elicited by STZ treatment presumably reflects a much greater increase in islet tissue. To localize PARP activation, we employed an autoradiographic technique monitoring the conversion of [^{33}P]NAD$^+$ to poly(ADP-ribose) polymer, termed PARIS. Radiolabeled polymer formation is markedly augmented by STZ treatment selectively in islet tissue (Fig. 6). This increase is substantially reduced in PARP

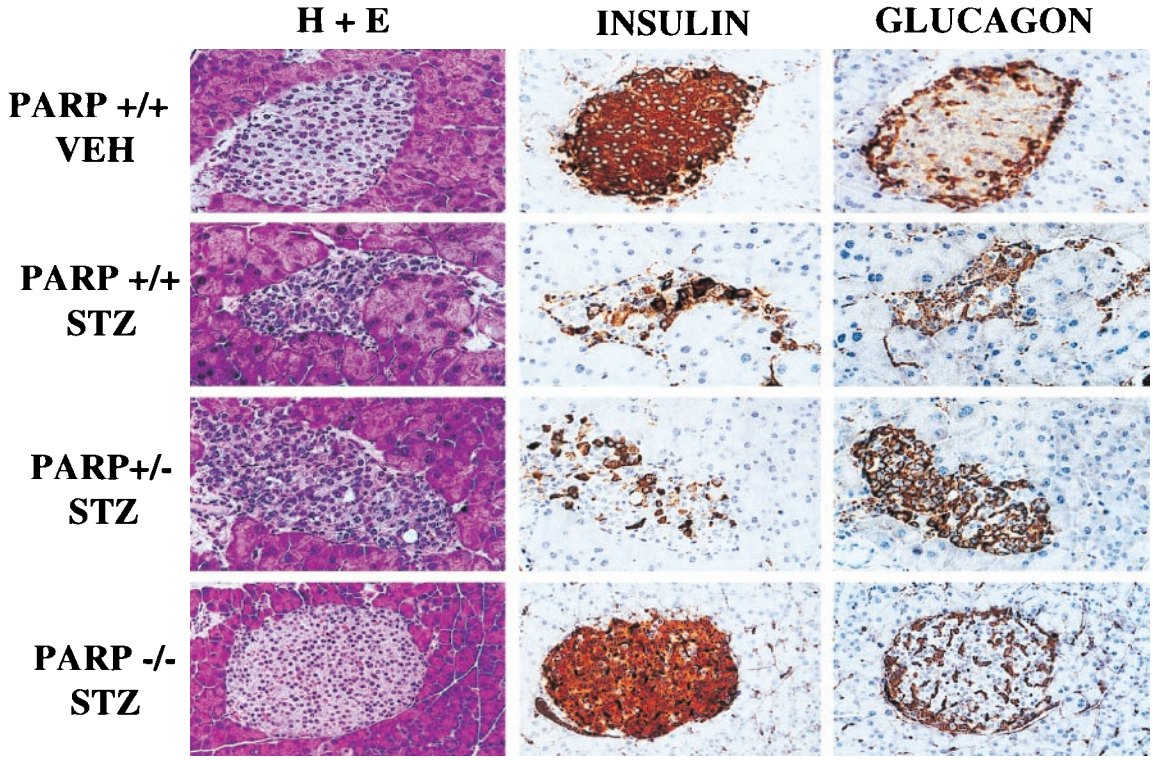

FIG. 3. Pancreatic islets are protected from STZ-induced B cell loss in PARP −/− mice. In wild-type and PARP +/− mice, pancreatic islets were small and distorted 6 weeks after a single i.p. injection of 200 mg/kg of STZ, as judged by staining with hematoxylin/eosin staining. Immunohistochemistry for insulin demonstrated that the majority of islet atrophy was caused by a marked loss of B cells. Glucagon immunoreactive cells appeared relatively spared but were no longer arranged peripherally in the islet. In contrast, islets from PARP −/− mice showed no evidence of atrophy (as judged by hematoxylin/eosin staining), B cell loss (as judged by insulin staining), or altered cellular arrangement (as judged by normal glucagon staining), and were histologically similar to vehicle treated PARP +/+ mice. The number and distribution of insulin and glucagon immunoreactive cells were also similar to those from islets from untreated controls. Results are representative of two trials with at least 5 mice per group.

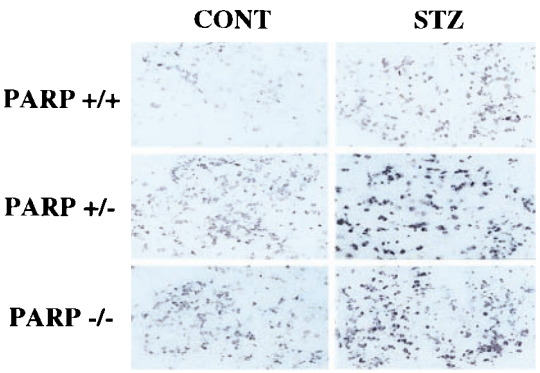

FIG. 4. STZ treatment damages DNA in PARP +/+, PARP +/−, and PARP −/− mice. PUNT+ labeling of DNA strand breaks in mouse pancreatic islet cells shows that i.p. injection of 200 mg/kg STZ elicits comparable DNA damage 5 days later in PARP +/+, PARP +/−, and PARP −/− mice. Baseline pancreatic islet cell DNA damage is higher in PARP +/− and PARP −/− mice than in PARP +/+ mice. These results are samples of at least five independent replications.

+/− islets and abolished in PARP −/− animals. Treatment of wild-type and PARP +/− pancreatic sections with benzamide, a PARP inhibitor, abolishes the autoradiographic signal, ensuring that radiolabel reflects PARP activity.

DISCUSSION

The primary finding of our study is that PARP −/− mice are fully protected from STZ-induced damage to pancreatic islet B cells. A variety of evidence supports the conclusion that pancreatic damage reflects massive activation of PARP in the islets sufficient to deplete NAD^+, the substrate of PARP, and then to deplete ATP, leading to cell death from energy loss. Although we have not directly monitored NAD^+ and ATP levels, such depletions occur in other models in which PARP inhibition protects from tissue damage. The protective paradigm of PARP inhibition after DNA damage has been demonstrated for numerous other models of cell death, including

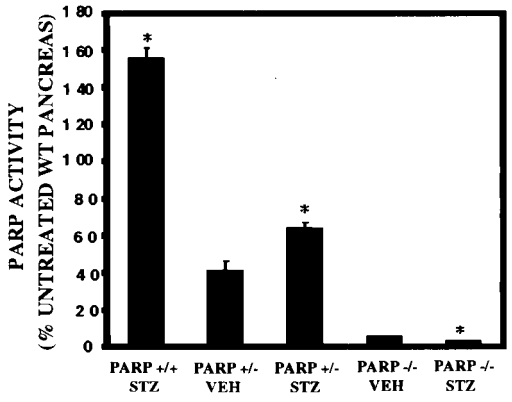

FIG. 5. PARP activation in mouse pancreas after STZ treatment. Wild-type pancreatic PARP activity is increased 5 days after treatment with 200 mg/kg of STZ. PARP −/− mice, however, show negligible basal PARP activity both before and 5 days after STZ treatment. PARP +/− mice have intermediate levels of basal PARP activity and PARP activation after STZ treatment. Values are means ± SEM for 3 trials of at least 5 mice per group. *, PARP +/+ STZ, significantly different from basal PARP +/+ pancreatic PARP activity, $P < 0.01$ (Student's *t* test). * PARP +/− STZ, significantly different from STZ-treated PARP +/+ pancreatic PARP activity, $P < 0.01$ (Student's *t* test). *, PARP −/− STZ, significantly different from STZ-treated PARP +/− pancreatic PARP activity, $P < 0.01$ (Student's *t* test).

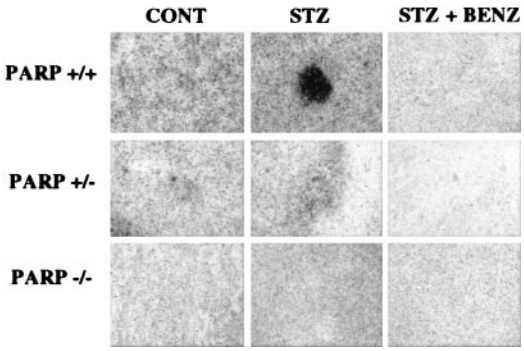

FIG. 6. PARP activation after STZ treatment is localized to islets in PARP +/+ pancreas. Emulsion was used to visualize microscopically *in situ* PARP activation using the PARIS detection technique. Pancreatic sections in this figure were adjacent to those used in Figs. 4 and 5. All PARIS sections shown were verified for the presence of islets through additional hematoxylin/eosin staining of adjacent pancreatic sections (data not shown). PARP +/+ pancreas shows some degree of basal PARP activity diffusely spread throughout the pancreas, which is greater than that seen in PARP +/− mice. There is a virtual absence of basal PARP activity in PARP −/− mice. Five days after i.p. injection of 200 mg/kg STZ, PARP +/+ mice show dramatic activation of PARP localized specifically to islet cells. This PARP activation corresponds to the induction of DNA damage shown in Fig. 4. After STZ treatment of PARP +/− mice, however, there is much less distinct and robust PARP activation in islet cells than in PARP +/+ mice. PARP −/− pancreas shows no PARIS signal after STZ treatment. Incorporation of the PARP inhibitor benzamide into the PARIS assay in pancreatic sections from STZ-treated PARP +/+ and PARP +/− mice abolishes PARIS signal, as this assay is specific for *in situ* PARP activity. PARIS signal in STZ-treated PARP −/− mice is unchanged with incorporation of benzamide into the PARIS assay.

cerebral ischemia (10–13, 26), myocardial ischemia (27–30), *N*-methyl-D-aspartic acid receptor-mediated excitotoxicity in the lung (31), methamphetamine neurotoxicity (32, 33), and MPTP toxicity (34–36). In all of these cases, a lack of PARP activity, through either genetic disruption or pharmacologic inhibition, provides impressive protection from cell death after DNA damage. In this study, we directly demonstrate activation of pancreatic islet PARP after STZ treatment with no activation in PARP −/− animals whose pancreata are devoid of PARP protein. STZ-induced DNA damage is the same in PARP −/− and wild-type animals, indicating that protection from islet destruction results from the lack of PARP activity in mutant mice.

Heterozygote (PARP +/−) mice display about half the wild-type levels of enzyme protein. They are partially protected from STZ diabetes with blood glucose 1 week after STZ treatment, the same as in STZ-treated PARP −/− mice. At 2 weeks, however, their blood glucose levels have increased to the high values of STZ-treated wild-type mice. When killed 2 weeks after STZ treatment, microscopic pancreatic damage is the same in heterozygote and wild type. Thus, the process of pancreatic damage in heterozygotes is presumably slowed. Ultimately, however, the damage is as great as it is in wild-type mice. In studies of focal cerebral ischemia, PARP +/− mice also display partial protection from brain damage (10, 11). In these stroke studies, animals were killed 1 day after occlusion of the middle cerebral artery. Whether the protection would diminish at later times, as it did in the STZ-treated heterozygotes, is unclear.

The finding of essentially total protection from pancreatic damage in PARP −/− animals is remarkable. PARP −/− mice are also protected from focal ischemic brain damage (10, 11) and myocardial ischemic damage (30). In two independent studies, protection from stroke damage was 50% (11) and 80% (10). Myocardial ischemic damage is reduced 40–50% in PARP −/− mice (30). What might account for these variable

levels of protection? One possibility is the existence of isoforms of PARP that are not lost in certain tissues of PARP −/− mice. By using the PARIS technique, we have detected 20–30% residual PARP activity in heart and lung of PARP −/− animals, although activity is abolished in brain and pancreas (data not shown). The residual PARP activity in the heart could account for the diminished myocardial protection. Cultured fibroblasts from PARP −/− mice display PARP activity ≈25% of wild-type levels, whereas cultured PARP −/− primary embryonic cells display ≈3% of wild-type levels (37). Very recently, novel isoforms of PARP have been identified (38, 39). The extent to which they contribute to PARP activity in various mammalian tissues has not been established.

In the absence of STZ treatment, we discovered substantial increases in DNA strand breaks in islet cells of PARP −/− and PARP +/− animals. These findings indicate that, under basal conditions, PARP participates in DNA repair, a finding that is consistent with recent evidence of its role in normal base excision repair (4–8). We do not know whether similar increases in DNA damage occur in other tissues of the mutant mice. Substantial increases in DNA damage in a wide range of PARP-deficient tissues would indicate a greater importance of PARP in normal physiology than has been implied by the relatively benign phenotype of PARP −/− animals.

The PUNT+ and PARIS techniques used here have enabled us to detect microscopically DNA strand breaks and PARP activation with considerable sensitivity and specificity as well as with high resolution. These procedures facilitated our observation of substantial levels of DNA damage in the pancreas under basal conditions. By using the same techniques, we have noted highly localized concentrations of DNA strand breaks and PARP activation in discrete brain regions (data not shown).

Our results imply that PARP activation and energy depletion are important elements in the pathophysiology of type I diabetes that is thought to be modeled by STZ treatment. How good of a model is STZ-induced diabetes? Type I diabetes is thought to arise after an autoimmune attack on pancreatic islets with activated macrophages eliciting much of the damage. In a model system using activated macrophages cocultured with pancreatic tissue, Burkart and Kolb (3) have demonstrated diminished damage in pancreatic tissue treated with inhibitors of either NO synthase or PARP. As described above, NO damages DNA and elicits cell death via subsequent activation of PARP. PARP inhibition protects pancreatic islet cells from NO-mediated cell death (14, 15), and cultured PARP −/− islet cells are resistant to NO- and other ROS-mediated energy depletion (16). Accordingly, STZ treatment may represent a meaningful model reflecting a role of PARP in the genesis of type I diabetic damage to the pancreas.

Recently, potent and selective inhibitors of PARP have been developed (10, 12, 40). These agents diminish brain damage after focal cerebral ischemia (10, 12) and myocardial ischemia (T. Walles, P. Wang, A.A.P., S.H.S., and J. L. Zweier, unpublished report). Conceivably, they may afford therapeutic benefit in type I diabetes. Our finding that the onset of hyperglycemia is delayed in PARP +/− mice suggests that even partial inhibition of PARP is therapeutic. In most patients, when type I diabetes is first diagnosed, the autoimmune process is ongoing, with the pancreas having sustained only a portion of its ultimate damage (41). Thus, treatment with PARP inhibitors at the time of diagnosis may slow disease progression. Nicotinamide is a soluble B group vitamin that serves as a precursor of NAD^+, a free radical scavenger, and a weak PARP inhibitor. Administration of nicotinamide prevents rodent diabetes after STZ administration (22) and also blocks the development of diabetes in the nonobese diabetic mouse, a model of spontaneous autoimmune diabetes (42). This nontoxic agent has displayed some limited beneficial effects in human diabetes (43–46) and is currently being evaluated as a prophylactic agent in first degree relatives of type I diabetic patients possessing islet cell antibodies (47).

We thank J. Zhang for helpful discussions. This work was supported by U.S. Public Health Service Grants MH18501 and DA00266 (S.H.S.), Research Scientist Award DA00074 (S.H.S.), Uniform Services University of the Health Sciences Grant R09271 (A.V.), and a grant from the Defense and Veteran's Head Injury Program (A.V.). Under an agreement between the Johns Hopkins University and Guilford, S.H.S. is entitled to a share of sales royalties related to PARP received by the University from Guilford. The University owns stock in Guilford with S.H.S. having an interest in the University Share under University policy. S.H.S. serves on the Board of Directors and the Scientific Advisory Board of Guilford, he is a consultant to the company, and he owns additional equity in Guilford. This arrangement is being managed by the University in accordance with its conflict-of-interest policies.

1. Mendola, J., Wright, J. R. & Lacy, P. E. (1989) *Diabetes* **38,** 379–385.
2. Rabinovitch, A., Suarez, W. L., Thomas, P. D., Strynadka, K. & Simpson, I. (1992) *Diabetologia* **35**, 409–413.
3. Burkart, V. & Kolb, H. (1993) *Clin. Exp. Immunol.* **93,** 273–278.
4. Menissier de Murcia, J., Niedergang, C., Trucco, C., Ricoul, M., Dutrillaux, B., Mark, M., Oliver, F. J., Masson, M., Dierich, A., LeMeur, M., *et al.* (1997) *Proc. Natl. Acad. Sci. USA* **94,** 7303–7307.
5. Masson, M., Niedergang, C., Schreiber, V., Muller, S., Menissier-de Murcia, J. & de Murcia, G. (1998) *Mol. Cell. Biol.* **18,** 3563–3571.
6. Leist, M., Single, B., Kunstle, G., Volbracht, C., Hentze, H. & Nicotera, P. (1997) *Biochem. Biophys. Res. Commun.* **233,** 518–522.
7. Wang, Z.-Q., Stingl, L., Morrison, C., Jantsch, M., Los, M., Schulze-Osthoff, K. & Wagner, E. F. (1997) *Genes Dev.* **11,** 2347–2358.
8. Oliver, F. J., de la Rubia, G., Rolli, V., Ruiz-Ruiz, M. C., de Murcia, G. & Murcia, J. M. (1998) *J. Biol. Chem.* **273,** 33533–33539.
9. Berger, N. A. (1985) *Radiat. Res.* **101,** 4–15.
10. Eliasson, M. J. L., Sampei, K., Mandir, A. S., Hurn, P. D., Traystman, R. J., Bao, J., Pieper, A. A., Wang, Z.-Q., Dawson, T. M., Snyder, S. H. & Dawson, V. L. (1997) *Nat. Med.* **3,** 1089–1095.
11. Endres, M., Wang, Z.-Q., Namura, S., Waeber, C. & Moskowitz, M. A. (1997). *J. Cereb. Blood Flow Metab.* **17**, 1143–1151.
12. Takahashi, K., Greenberg, J. H., Jackson, P., Maclin, K. & Zhang, J. (1997) *J. Cereb. Blood Flow Metab.* **17**, 1137–1142.
13. Tokime, T., Nozaki, K., Sugino, T., Kikuchi, H., Hashimoto, N. & Ueda, K. (1998) *J. Cereb. Blood Flow Metab.* **18,** 991–997.
14. Radons, J., Heller, B., Burkle, A., Hartmann, B., Rodriguez, M. I., Kroncke, K. D., Burkart, V. & Kolb, H. (1994) *Biochem. Biophys. Res. Commun.* **199,** 1270–1277.
15. Inada, C., Yamada, K., Takane, N. & Nonaka, K. (1995) *Life Sci.* **56,** 1467–1474.
16. Heller, B., Wang, Z.-Q., Wagner, E. F., Radons, J., Burkles, A., Fehsel, K., Burkart, V. & Kolb, H. (1995) *J. Biol. Chem.* **270,** 11176–11180.
17. Rerup, C. C. (1970) *Pharmacol. Rev.* **22,** 485–518.
18. Agarwal, M. K. (1980) *FEBS Lett.* **120,** 1–3.
19. Yamamoto, H., Uchigata, Y. & Okamoto, H. (1981) *Nature (London)* **294,** 284–286.
20. Ho, C.-K. & Hashim, S. A. (1972) *Diabetes* **21,** 789–793.
21. Hinz, M., Katsilambros, N., Maier, V., Schatz, H. & Pfeiffer, E. F. (1973) *FEBS. Lett.* **30**, 225–228.
22. Schein, P. S., Cooney, D. A. & Vernon, M. L. (1967) *Cancer Res.* **27,** 2324–2332.
23. Chen, J., Jin, K., Chen, M., Pei, W., Kawaguchi, K., Greenberg, D. A. & Simon, R. P. J. (1997) *Neurochemistry* **69,** 232–245.
24. Blaschke, A. J., Staley, K. & Chun, J. (1996) *Development (Cambridge, U.K.)* **122,** 1165–1174.
25. Rossini, A. A., Like, A. A., Chick, W. L., Appel, M. C. & Cahill, G. F., Jr. (1977) *Proc. Natl. Acad. Sci. USA* **74**, 2485–2489.
26. Zhang, J., Dawson, V. L., Dawson, T. M. & Snyder, S. H. (1994) *Science* **263**, 687–689.

27. Gilad, E., Zingarelli, B., Salzman, A. L. & Szabo, C. (1997) *J. Mol. Cell. Cardiol.* **29**, 2585–2597.
28. Thiemermann, C., Bowes, J., Myint, F. P. & Vane, J. R. (1997) *Proc. Natl. Acad. Sci. USA* **94**, 679–683.
29. Bowes, J., Ruetten, H., Martorana, P. A., Stockhausen, H. & Thiemermann, C. (1998) *Eur. J. Pharmacol.* **359,** 143–150.
30. Zingarelli, B., Salzman, A. L. & Szabo, C. (1998) *Circ. Res.* **83,** 85–94.
31. Said, S. I., Berisha, H. I. & Pakbaz, H. (1996) *Proc. Natl. Acad. Sci. USA* **93**, 4688–4692.
32. Sheng, P., Cerruti, C., Ali, S. & Cadet, J. L. (1994) *Ann. N.Y. Acad. Sci.* **801**, 74–186.
33. Cosi, C., Chopin, P. & Marien, M. (1996) *Brain Res.* **735,** 343–348.
34. Zhang, J., Pieper, A. A. & Snyder, S. H. (1995) *J. Neurochem.* **65,** 1411–1414.
35. Cosi, C., Chopin, P. & Marien, M. (1996) *Brain Res.* **729,** 264–269.
36. Cosi, C. & Marien, M. (1998) *Brain Res.* **809,** 58–67.
37. Shieh, W. M., Ame, J.-C., Wilson, M. V., Wang, Z.-Q., Koh, D. W., Jacobson, M. K. & Jacobson, E. L. (1998) *J. Biol. Chem.* **273,** 30069–30072.
38. Babiychuk, E., Cottrill, P. B., Storozhenko, S., Fuangthong, M., Chen, Y., O'Farrell, M. K., Van Montagu, M., Inze, D. & Kushnir, S. (1998) *Plant J.* **15,** 635–645.
39. Smith, S., Giriat, I., Schmitt, A. & de Lange, T. (1998) *Science* **282,** 1484–1487.
40. Griffin, R. J., Srinivasan, S., Bowman, K., Calvert, A. H., Curtin, N. J., Newell, D. R., Pemberton, L. C. & Golding, B. T. (1998) *J. Med. Chem.* **41,** 5247–5256.
41. Gale, E. A. M. (1996) *Horm. Res.* **45,** 40–43.
42. Elliot, R. B., Pilcher, C. C., Stewart, A., Fergusson, D. & McGregor, M. A. (1993) *Ann. N.Y. Acad. Sci.* **696**, 333–341.
43. Vague, P., Vialettes, B., Lassman-Vague, V. & Vallo, J. J. (1987) *Lancet* **i,** 619-620.
44. Mendola, G., Casamitjana, R. & Gomis, R. (1989) *Diabetologia* **32,** 160–162.
45. Vague, P., Picq, R., Bernal, M., Lassman-Vague, V. & Vialettes, B. (1989) *Diabetologia* **32**, 316–321.
46. Mandrup-Poulson, T., Remiers, J. I., Andersen, H. U., Pociot, F., Karlsen, A. E., Bjerre, U. & Nerup, J. (1993) *Diabetes Metab. Rev.* **9,** 295–309.
47. Gale, E. A. M. (1996) *J. Pediatr. Endocrinol. Metab.* **9,** 375–379.